Comparisons of ZnO codoped by group IIIA elements (Al, Ga, In) and N: a first-principle study*

Li Ping(李 平)[a)†], Deng Sheng-Hua(邓胜华)[b)], Zhang Li(张 莉)[a)], Yu Jiang-Ying(余江应)[a)], and Liu Guo-Hong(刘果红)[a)]

[a)] *Department of Mathematics and Physics, Anhui University of Architecture, Hefei* 230022, *China*
[b)] *School of Physics and Nuclear Energy Engineering, Beihang University, Beijing* 100191, *China*

(Received 18 April 2010; revised manuscript received 25 June 2010)

The electronic structures and effective masses of the N mono-doped and Al–N, Ga–N, In–N codoped ZnO system have been calculated by a first-principle method, and comparisons among different doping cases are made. According to the results, the impurity states in the codoping cases are more delocalised compared to the N mono-doping case, which means a better conductive behaviour can be obtained by codoping. Besides, compared to the Al–N and Ga–N codoping cases, the hole effective mass of In–N codoped system is much smaller, indicating the p-type conductivity can be more enhanced by In–N codoping.

Keywords: first-principles, ZnO, conductivity, doping
PACC: 7115H, 7115M

1. Introduction

As a new type II–VI compound semiconductor, ZnO has a wide direct gap of 3.37 eV at room temperature and large exciton binding energy of 60 meV, and it has attracted much attention for its wide applications in transparent conducting contacts, blue lasers and light emitting diodes.[1,2] In order to fabricate ZnO-based optoelectronic devices, both n- and p-type ZnO are needed. It is easy to obtain good conductive n-type ZnO by mono-doping the group IIIA elements as donors, but ZnO with good p-type conductivity is difficult to fabricate, which has impeded the developments and applications of the ZnO-based devices.

To obtain p-type ZnO, mono-doping is a common method, and in this method the group VA elements are good candidates as dopants. In recent years, N,[3−9] P,[10−12] As[13,14] and Sb[15,16] have been studied in experiment as mono-dopants to obtain p-type ZnO, and some promising results are reported in the corresponding literatures cited above. Compared to the mono-doping method, codoping approach seems to be more attractive in the realisation of p-type ZnO, and it has attracted more and more attention in recent years. The group IIIA–N elements are frequently-used candidates for codoping, for example, Al–N,[17−20] Ga–N,[21] and In–N[22,23] have been studied individually. Though many promising experimental results have also been reported in the codoping process, the results depend strongly on the experimental situations, conditions and the adopted methods. In theory, much work is also done about the mono-doping and codoping approach[24−29] by first-principle method, but little of them make comparisons of different dopants. In order to find better ways or better candidates to realise ideal p-type ZnO, comparisons of different dopants in theory are necessary. In this paper, comparisons of the differences among N mono-doped and Al–N, Ga–N, In–N codoped ZnO will be made by a first-principle calculation. During the discussions, the doping properties, especially the conductive properties will be paid special attention.

This paper is organised as follows: Firstly, the model and method are introduced. Secondly, the electronic structures and effective masses of carriers are calculated in the N mono-doping case and the Al–N, Ga–N, In–N codoping cases, and then comparisons and discussions about them are made; finally, conclusions are drawn.

*Project supported by the Special Foundation for Young Scientists of Anhui Province, China (Grant No. 2009SQRZ097ZD) and the Foundation of Anhui University of Architecture (Grant No. 20070601).
†Corresponding author. E-mail: liping@ss.buaa.edu.cn; liping@aiai.edu.cn
© 2010 Chinese Physical Society and IOP Publishing Ltd

2. Model and method

The ideal ZnO has a hexagonal wurtzite structure with a space group symmetry of $P63/mc$ and $C6v$-4, each primitive cell contains two O atoms and two Zn atoms, and the cell parameters are $a = b = 0.3249$ nm, $c = 0.5206$ nm.[30] Based on the primitive cell, a 2×2×2 ZnO supercell is constructed and shown in Fig.1, and sites A1 to A5 are labeled for further description. In the N mono-doping case, one N substitutes for one O of A5 site as an acceptor. In the codoping cases, the group IIIA element (Al, Ga, In) substitutes for one Zn of A1 site as a donor, and two N atoms substitute symmetrically for two neighbouring O of A2 and A3 sites as acceptors (mode I). The choice of mode I is because, according to our calculation, this mode has slightly lower energy than the A1,A2 and A4 substituting codoping mode (mode II).

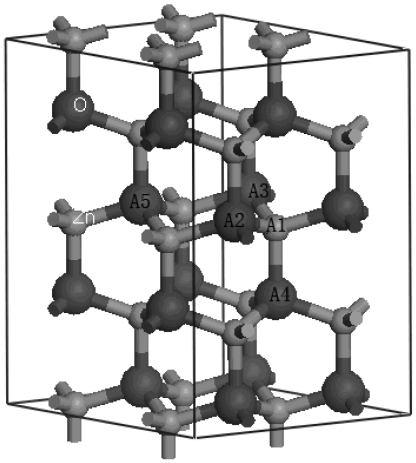


Fig. 1. Supercell of ZnO.

First-principle calculations based on the density functional theory (DFT) were performed using the Vienna *ab initio* simulation package (VASP) code.[31] During our calculations, projector augmented wave (PAW) pseudo-potentials[32] were used to describe the interactions between the atomic nucleus and valence electrons, the generalised gradient approximation (GGA)[33] was used to describe the exchange–correlation energy among electrons, and a 4×4×2 k-point mesh was employed for the Brillouin zone integration of the 32-atom supercell. The energy cutoff was 520 eV, which had been confirmed to be large enough. The breaking condition for ionic relaxation in total energy was 10^{-5}eV and that in force acting on each ion was 0.01 eV/Å (1 Å=0.1 nm). The calculated cell parameters in our work are $a = b = 0.3199$ nm, $c = 0.5216$ nm, which are in good agreement with the experimental values.[30]

3. Results and discussions

3.1. Comparisons of the electronic structures

Table 1 lists the bond length of the undoped, mono-doped and codoped ZnO calculated in our work, together with the energy differences (ΔE) of the system before and after doping. Taking N doping as an example to explain ΔE: when N is doped into the ZnO supercell, the process can be described as follows:

$$\mathrm{N} + \mathrm{Zn_{16}O_{16}} = \mathrm{Zn_{16}O_{15}N} + \mathrm{O}, \tag{1}$$

then

$$\Delta E = E(\mathrm{Zn_{16}O_{15}N}) + E(\mathrm{O}) - E(\mathrm{N}) - E(\mathrm{Zn_{16}O_{16}}), \tag{2}$$

where $E(\mathrm{Zn_{16}O_{15}N})$ stands for the energy of $\mathrm{Zn_{16}O_{15}N}$ system and so on. According to the definition, $-\Delta E$ for the pure primitive ZnO is the binding energy, and our result (7.23 eV) is in good agreement with the reported value of 7.20 eV.[34]

Table 1. Energy differences (ΔE) and bond length (L_b) in various doping cases, in units of eV and Å respectively.

	pure ZnO	ZnO(N)	ZnO(Al–N)	ZnO(Ga–N)	ZnO(In–N)
ΔE	–7.23	2.36	–2.45	0.58	2.72
L_b	O-Zn[1]: 1.98	N-Zn[1]: 1.93	O-Al[1]:1.82	O-Ga[1]:1.93	O-In[1]:2.13
	O-Zn[2]:1.98	N-Zn[2]: 1.94	O-Al[2]:1.82	O-Ga[2]:1.92	O-In[2]:2.10
			N-Al[2]:1.87	N-Ga[2]:1.90	N-In[2]:2.09

[1]-Parrallel to c axis.

[2]-Perpendicular to c axis.

From Table 1, in the N-mono doping, Al–N and Ga–N codoping cases, the impurity-related bonds become smaller no matter whether they are in the directions of parallel or perpendicular to c axis compared with the pure ZnO situation, indicating a strong interaction between the corresponding atoms. On the contrary, the In–related bonds become larger compared to the O–Zn bond in pure situation, which can be explained by the bigger difference between the atomic radii of In and Zn. From the viewpoint of energy, it can be seen that the energy increases after N-doping, indicating an unstable state of the codoping system. While in the codoping, ΔE increases from Al to In, this is opposite to the changes of impurity-related bond length. In the Al–N codoping, ΔE is negative, and it can be due to the strong attraction among the N, Al and O, which is in agreement with the small bond length. In the Ga–N codoping, the bond length becomes larger and the corresponding attraction decreases too, so the energy of the system increases and then ΔE turns to be positive value. In the In–N codoping, the corresponding attraction decreases further and the larger distortion of lattice also increases the energy of the codoping system, so ΔE increases further. It should be pointed out especially that, though ΔE is listed and discussed here, it should not be used to infer the solubility of dopants, which is determined by the formation energy according to the experimental conditions.

Figures 2(a)–2(b) show the charge density contour plots of the pure ZnO and N mono-doped ZnO, respectively. It can be seen that in pure ZnO, electrovalent bonds mixed with small amount of covalent property are formed between O and Zn. In the N-doping case, the chemical bonds between N and Zn are similar to that between O and Zn.

Figures 3(a)–3(c) show the charge density contour plots of the dopants in the three codoping cases. Compared with Fig. 2, the changes in codoping cases are obvious. The contour plots in Fig. 3 (a) to 3(c) show evidently directional properties, indicating that Al–N, Ga–N and In–N bonds with strong covalent properties are formed between dopants in the codoping.

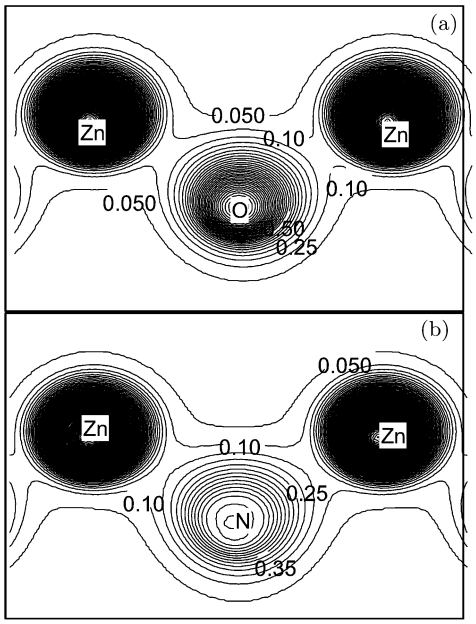


Fig. 2. Charge density contour plots: (a) pure ZnO and (b) N mono-doping. The interval of the contour lines is 0.05 e/Å^3.

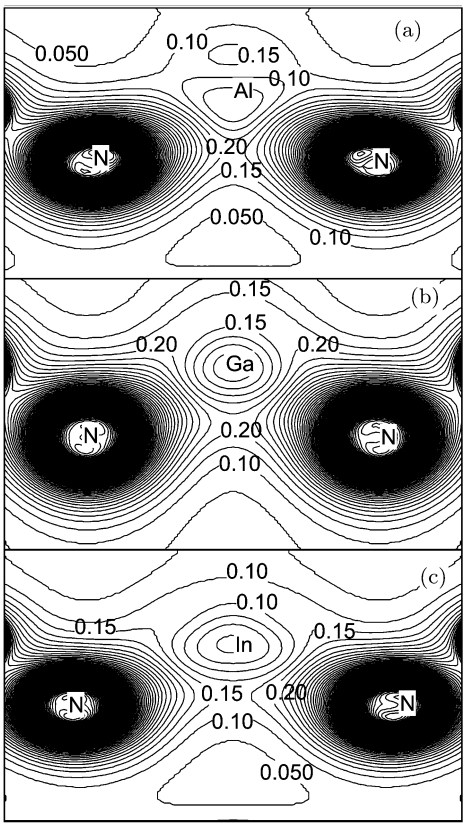


Fig. 3. Charge density contour plots: (a) Al–N codoping, (b) Ga–N codoping, and (c) In–N codoping. The interval between the contour lines is 0.05 e/Å^3.

Figures 4 and 5 show the calculated band structures (BS) and total density of states (TDOS) of pure

ZnO respectively, where the Fermi-level has been set to be zero in this paper. In the BS plots, the extreme values of the conduction band and the valence band are at the same k-point (G), indicating that ZnO is a direct gap semiconductor. Though the calculated band gap is underestimated as 1.05 eV, only 31% of the experimental data, which is a common problem of local density approximation (LDA) or GGA, it is in good agreement with other data calculated by the same method.[35,36] The BS and DOS have been discussed so much in many first-principle related literatures,[25,36] so we will not pay more attention to them.

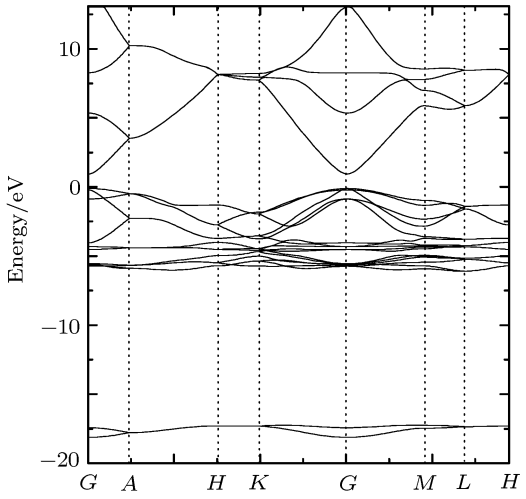


Fig. 4. BS of ZnO.

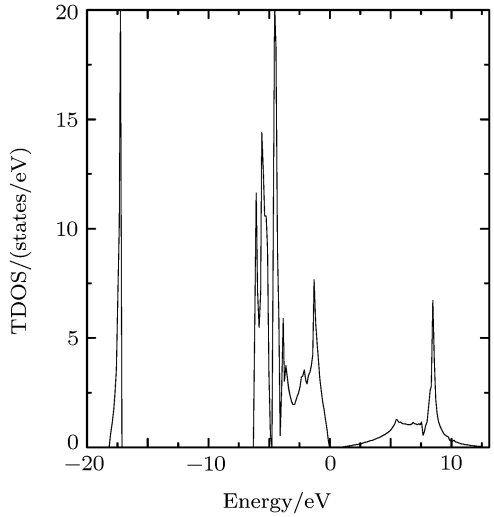


Fig. 5. TDOS of ZnO.

Figures 6(a) and 6(b) show the TDOS and the partial density of states (PDOS) of N near the Fermi-level in the N mono-doping case respectively. Compared to the pure situation shown in Fig. 5, an impurity state appears near the top of the valence band, which means the realisation of ZnO with p-type conductivity. Together with the PDOS of N in Fig. 6(b), it can be judged that the impurity state is mainly contributed by the N-p orbits, and the contributions of the N-s orbits are negligible. However, the impurity state is local and sharp near the Fermi-level, perhaps meaning a poor conductive behaviour in the N mono-doped ZnO system.

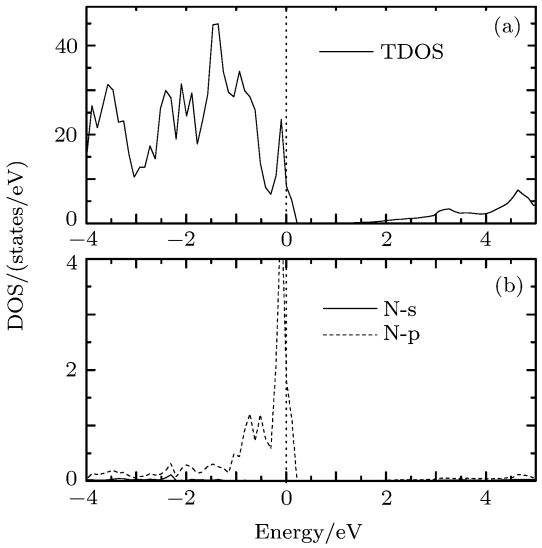


Fig. 6. (a) TDOS of ZnO doped with N. (b) PDOS of N.

Figures 7–9 show the TDOS and PDOS of dopants near the Fermi-level in the Al–N, Ga–N and In–N codoping cases respectively. First, from the three figures it seems to be suitable to judge that the impurity levels are formed between the energy gap of the host ZnO lattice, though the resolution of the impurity levels from the top of the valence band of the host is somewhat ambiguous. Since these impurity levels appear between the gaps or near the Fermi-levels, it can be judged that p-type ZnO can be obtained by codoping method. Secondly, it is obvious that the plots in Figs. 7–9 are very similar. Despite of this, the states of N-p in codoping cases near the Fermi-level shown in Figs. 7(b)–9(b) are much delocalised compared to the N mono-doping case in Fig. 6(b), which implies better conductive behaviours in the codoped ZnO system. And finally, the PDOSs of Al, Ga and In in Figs. 7(a)–9(a) extend deeply into the valence band, but are small at the Fermi-level. On the contrary, the PDOSs of N in the three codoping cases are not so delocalised, but are much larger at Fermi-level, so the influence of acceptors is dominant, which can also explain the p-type conductive behaviours of the codoped ZnO system.

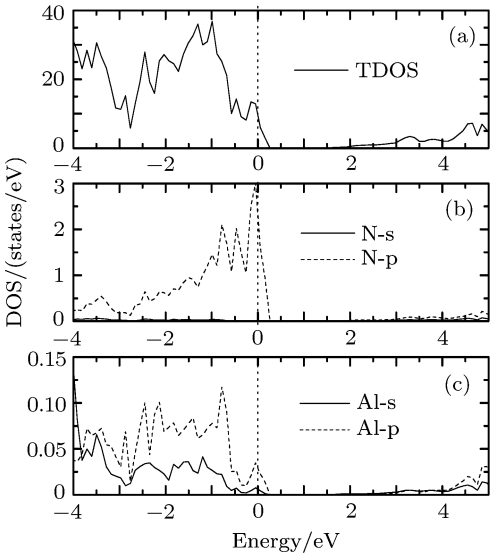


Fig. 7. (a) TDOS of ZnO codoped with N and Al. (b) PDOS of N. (c) PDOS of Al.

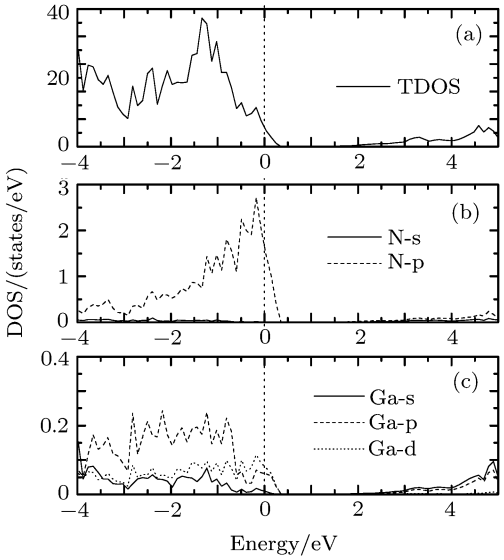


Fig. 8. (a) TDOS of ZnO codoped with N and Ga. (b) PDOS of N. (c) PDOS of Ga.

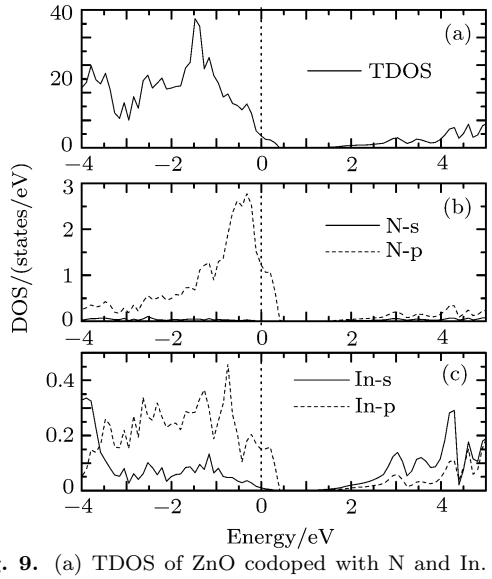


Fig. 9. (a) TDOS of ZnO codoped with N and In. (b) PDOS of N. (c) PDOS of In.

Figures 10(a)–10(d) show the band structures near the Fermi-level of N mono-doped and Al–N, Ga–N, In–N codoped ZnO respectively. It can be seen that the main differences in the four plots appear near the Fermi-level. In the mono-doping case shown in Fig. 10(a), the impurity bands are hybridised with the native bands of ZnO, while in the codoping cases, the impurity bands are apart from the native bands of ZnO, especially in the Al–N codoping case.

From the discussions above, it can be concluded that p-type ZnO can be obtained both by the mono-doping and the codoping methods, and it seems that the codoping is superior to the mono-doping. But the codoping DOSs are so similar to each other in the three cases, it is not easy to determine which dopant is more preferable. To make further comparisons among the three codoping cases, the effective masses of carriers are calculated.

3.2. Comparisons of the effective masses

Effective mass is one of the fundamental quantities in semiconductor physics, which can help us to understand a wide range of phenomena, in particular, the transport phenomena, so the effective masses of electrons and holes are calculated in our work. According to the solid theory, neglecting the cross terms, the effective mass of carriers at the conduction band minimum or valence band maximum can be expressed as follows:

$$m_i = \left(\frac{h}{2\pi}\right)^2 / \frac{\partial^2 E}{\partial k_i^2}, \tag{3}$$

where only the absolute value of the effective mass is adopted. In the formula, i stands for x, y or z, where directions x and y correspond to GM, and direction z corresponds to GA in the first Brillouin zone.

During our calculations of effective masses, 50-kpoints are used along the GA and GM directions in the reciprocal space, which have been confirmed to be more enough. First of all, the second derivative at gamma point is fitted along GA and GM directions respectively, and then the effective masses can be obtained according to formula (3). The calculated effective masses of pure ZnO are shown in Table 2 together with experimental values and other calculated data based on LDA. In this table, the subscripts c and v stand for the conduction band and the valence band, x and z mean directions of x and z respectively, and m_0 is the rest mass of the electron. The calculated results in our work agree well with the experimental data, perhaps, the GGA plays an important role here.

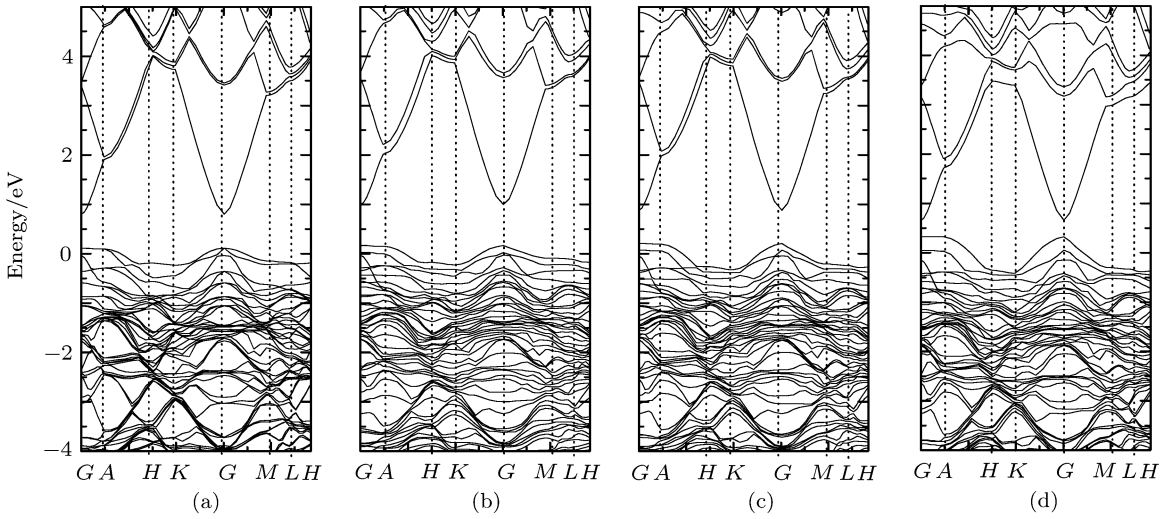


Fig. 10. Band structures in (a) N mono-doping, (b) Al–N, (c) Ga–N and (d) In–N codoping cases.

Table 2. Effective masses of pure ZnO in units of m_0.

	our data based on GGA	LDA data[37,38]	experimental data[37]
m_{cz}	0.22	0.18	0.21
m_{cx}	0.23	0.21	0.24
m_{vz}	3.09	–	–
m_{vx}	2.68	–	–

The effective masses in the three codoping cases are listed in Table 3, in which the values of N mono-doped and Ga–N codoping cases agree well with the values reported in Ref. [39]. However, no experimental or other calculated data for the Al–N and In–N codoping cases have been found so as to be compared with our data. By comparing the data listed in Table 3 and Table 2, it can be seen that the effective masses of electrons in the undermost conduction band are almost unchanged, but the effective masses of holes in the uppermost valence band change a lot. Besides, an interesting phenomenon should also be noted that m_{vx} is much smaller in the codoping cases than that in the N mono-doping case. In order to find whether this phenomenon is related to the codoping mode or not, the effective masses of mode II substitutions are studied for Al–N codoping, and the same thing happens. The calculated m_{vx} is $0.47m_0$ for Al–N in mode II codoping, which is only $0.01m_0$ larger than that in mode I listed in Table 3 and is still much smaller than that in the N mono-doping case. So it seems that the enormous difference of m_{vx} between mono-doping and codoping is not induced by the codoping mode.

Table 3. Effective masses of ZnO with dopants and ionisation energy related to m_d (E_i) in units of m_0 and meV, respectively.

dopants	N	Al–N	Ga–N	In–N
m_{cz}	0.17	0.18	0.17	0.16
m_{cx}	0.20	0.20	0.20	0.19
m_{vz}	11.31	10.49	17.44	21.49
m_{vx}	2.46	0.46	0.32	0.22
m_c	3.33	0.68	0.48	0.33
m_d	4.09	1.30	1.21	1.01
E_i	742	236	219	183

We can describe and compare the effective masses simply by using an average effective mass of conductivity (m_c) or of DOS (m_d) as follows:

$$\frac{1}{m_c} = \frac{1}{3}\left(\frac{2}{m_x} + \frac{1}{m_z}\right), \tag{4}$$

$$m_d = \left(m_x^2 m_z\right)^{1/3}. \tag{5}$$

According to the formulas, the calculated average effective masses m_c and m_d of carriers in the mono-doping and codoping cases are also listed in Table 3. The dopants in our work have one more or less electron than the native atoms, so according to the solid theory, they can be treated as hydrogenic. In this sim-

ple model, the ionisation energy ($E_{\rm i}$) of acceptor can be estimated from $m_{\rm d}$ as follows:[39]

$$E_{\rm i} = \frac{m_{\rm d} E_0}{m_0 \varepsilon_{\rm r}^2}, \tag{6}$$

where the values of $E_{\rm i}$ related to $m_{\rm d}$ are also listed in Table 3 too. And the area of ground state wavefunctions of hydrogenic impurity can be estimated by

$$a = \frac{\varepsilon_{\rm r} m_0 a_0}{m_{\rm d}}, \tag{7}$$

where $\varepsilon_{\rm r} = 8.66$ is the relative permittivity of the host ZnO crystal,[40] $E_0 = -13.6$ eV is the ground energy of hydrogen atom, and a_0=0.52 angstrom is the Bohr radius.

We have noted that the experimental ionisation energy of substitutional N at an O site is around 200 meV, for instance, 209±3 meV,[41] 170–200 meV,[6] and a calculated acceptor ionisation energy about 195±10 meV in codoping cases is conferred to be likely due to the substitutional N.[42] From Table 3, the values of $E_{\rm i}$ in the N mono-doping case are obvious larger than the values referred above; we think this deviation may come from the deficiency of LDA or GGA in estimating the band gap of semiconductors. Taking into consideration the deviation, the effective masses of $m_{\rm c}$ and $m_{\rm d}$ in the N mono-doping cases listed in Table 3 agree well with other calculated values of $3.20m_0$ and $4.04m_0$[39] respectively. However, the acceptor ionisation energy in Table 3 in the three codoping cases are in agreement with the reported values.[6,41,42] From the table, the ionisation energy decreases from Al–N to In–N codoping cases.

According to formulas (6) and (7), a smaller effective mass means a smaller ionisation energy and a longer free path, which are in favour of good conductivity. From Table 3, it is obvious that the average effective mass in In–N codoping case is smaller than that in other codoping cases, so it can be concluded that the conductive ability will be much enhanced by In–N codoping.

4. Conclusions

The electronic structures and effective masses of N mono-doped, Al–N, Ga–N and In–N codoped ZnO systems have been calculated by a first-principle method. On the one hand, the impurity levels are rather local near the Fermi-level in the N mono-doping case, while in the Al–N, Ga–N and In–N codoping cases, the impurity levels become delocalised, and the DOSs in the three codoping cases are very similar. On the other hand, the effective mass in In–N codoping case is smaller than that in other codoping cases.

So according to the results, we can draw two conclusions: the first one is that the codoping method has advantages over the mono-doping to realise p-type ZnO, and the second one is that p-type conductivity of ZnO can be more enhanced by In–N codoping compared to other codoping cases.

References

[1] Klingshirn C 2007 *Chem. Phys. Chem.* **8** 782

[2] Tang Z K, Wong G K, Kawasaki P, Kawasaki M, Ohtomo A, Koinuma H and Segawa Y 1998 *Appl. Phys. Lett.* **72** 3270

[3] Xu W Z, Ye Z Z, Zhou T, Zhao B H, Zhu L P and Huang J Y 2004 *J. Cryst. Growth* **265** 133

[4] Kang H S, Ahn B D, Kim J H, Kim G H, Lim S H, Chang H W and Lee S Y 2006 *Appl. Phys. Lett.* **88** 202108

[5] Du G, Ma Y, Zhang Y and Yang T 2005 *Appl. Phys. Lett.* **87** 213103

[6] Look D C, Reynolds D C, Litton C W, Jones R L, Eason D B and Cantwell G 2002 *Appl. Phys. Lett.* **81** 1830

[7] Rommeluere J F, Svob L, Jomard F, Mimila-Arroyo J, Lusson A, Sallet V and Marfaing Y 2003 *Appl. Phys. Lett.* **83** 287

[8] Xu W Z, Ye Z Z, Zeng Y J, Zhu L P, Zhao B H, Jiang L, Lu J G, He H P and Zhang S B 2006 *Appl. Phys. Lett.* **88** 173506

[9] Tsukazaki A, Ohtomo A, Onuma T, Ohtani M, Makino T, Sumiya M, Ohtani K, Chichibu S, Fuke S, Segawa Y, Ohno H, Koinuma H and Kawasaki M 2005 *Nat. Mater.* **4** 42

[10] Yu Zh G, Wu P and Gong H 2006 *Appl. Phys. Lett.* **88** 132114

[11] Xiu F X, Yang Z, Mandalapu L J, Liu J L and Beyermann W P 2006 *Appl. Phys. Lett.* **88** 052106

[12] Vaithianathan V, Lee B T and Kima S S 2006 *J. Appl. Phys.* **98** 043519

[13] Vaithianathan V, Lee B T, Chang Ch H, Asokan K and Kim S S 2006 *Appl. Phys. Lett.* **88** 112103

[14] Vaithianathan V, Lee B T and Kim S S 2005 *Appl. Phys. Lett.* **86** 062101

[15] Mandalapu L J, Yang Z, Xiu F X, Zhao D T and Liu J L 2006 *Appl. Phys. Lett.* **88** 092103

[16] Xiu F X, Yang Z, Mandalapu L J, Zhao D T, Liua J L and Beyermann W P 2005 *Appl. Phys. Lett.* **87** 152101

[17] Yuan G D, Ye Z Z, Zhu L P, Qian Q, Zhao B H and Fan R X 2005 *Appl. Phys. Lett.* **86** 202106

[18] Bian J M, Li X M, Zhang C Y and Chen L D 2004 *Appl. Phys. Lett.* **84** 3783
[19] Dai L P, Deng H, Chen J J and Wei M 2007 *Solid State Commun.* **143** 378
[20] Zhu Q Y, Ye Z Z, Yuan G D, Huang J Y, Zhu L P, Zhao B H and Lu J G 2006 *Appl. Surf. Sci.* **253** 1903
[21] Kumar M, Kim T H, Kim S S and Lee B T 2006 *Appl. Phys. Lett.* **89** 112103
[22] Chen L L, Lu J G, Ye Z Z, Lin Y M, Zhao B H, Ye Y M, Li J S and Zhu L P 2005 *Appl. Phys. Lett.* **87** 252106
[23] Cao Y, Miao L, Tanemura S, Tanemura M, Kuno Y and Hayashi Y 2006 *Appl. Phys. Lett.* **88** 251116
[24] Huang G Y, Wang Ch Y and Wang J T 2009 *Scripta Materialia* **61** 324
[25] Shen Y Q, Mi L, Xu X F, Wu J D, Wang P N, Ying Zh F and Xu N 2008 *Solid State Commun.* **148** 301
[26] Duan X Y, Zhao Y J and Yao R H 2008 *Solid State Commun.* **147** 194
[27] Zuo C Y, Wen J and Bai Y L 2010 *Chin. Phys.* B **19** 047101
[28] Liu X C, Lu ZH and Zhang F M 2010 *Chin. Phys.* B **19** 027502
[29] Huang G Y, Wang C Y and Wang J T 2010 *Chin. Phys.* B **19** 013101
[30] Vispute R D, Talyansky V, Choopun S, Sharma P P, Venkatesan T, He M, Tang X, Halpern J B, Spencer M G, Li Y X and Salamanca-Riba L G 1998 *Appl. Phys. Lett.* **73** 348
[31] Kress G and Furthmuller J 1996 *Phys. Rev.* B **54** 11169
[32] Hamarm D R, Schhter M and Chiang C 1979 *Phys. Rev. Lett.* **43** 1494
[33] Perdew J P, Chevary J A, Vosko S H, Jackson K A, Perderson M R and Singh D J 1992 *Phys. Rev.* B **46** 6671
[34] Schleife A, Fuchs F, Furthmuller J and Bechstedt F 2006 *Phys. Rev.* B **73** 245212
[35] Wardle M G, Goss J P and Briddon P R 2006 *Phys. Rev. Lett.* **96** 205504
[36] Imai Y, Watanabe A and Shimono I 2003 *J. Mater. Sci. –Mater. Electron.* **14** 149
[37] Oshikiri M, Aryasetiawan F, Imanaka Y and Kido G 2002 *Phys. Rev.* B **66** 125204
[38] Oshikiri M, Imanaka Y, Aryasetiawan F and Kido G 2001 *Physica* B **298** 472
[39] Zhou C and Kang J 2004 13th *International Conference on Semiconducting and Insulating Materials SIMC-XIII-2004*, Beijing, September, pp81–84
[40] Pearton S J, Norton D P, Ip K, Heo Y W and Steiner T 2004 *J. Vac. Sci. Technol.* B **22** 932
[41] Wang L and Giles N C 2004 *Appl. Phys. Lett.* **84** 3049
[42] Thonke K, Gruber Th, Teofilov N, Schönfelder R, Waag A and Sauer R 2001 *Physica* B **308–310** 945